Reading the ripples of confined surface-state electrons: Profiles of constant integrated local density of states

Marina Pivetta,[1] Fabien Silly,[1] François Patthey,[1] Jonathan P. Pelz,[2] and Wolf-Dieter Schneider[1]
[1]*Institut de Physique de la Matière Condensée, Université de Lausanne, CH-1015 Lausanne, Switzerland*
[2]*Department of Physics, The Ohio State University, Columbus, Ohio 43210*
(Received 16 January 2003; published 5 May 2003)

Atomically resolved scanning tunneling microscope images of a Ag(111) surface are presented, which simultaneously display standing-wave patterns arising from the confinement of surface-state electrons to nanoscale terraces. We show how the energy-dependent patterns develop from the superposition of allowed wave functions in the quantum box. A simple free-electron model is already sufficient to identify all major features in differential conductance (dI/dV) maps and constant current topographic images, which both result from the superposition of up to eight allowed states. These results illustrate how the difference between dI/dV and topographic measurements can be pronounced already for very low bias voltages. An analysis of dI/dV spectra measured on large defect-free terraces yields a surface-state lifetime width of $\Gamma = 4.9 \pm 0.2$ meV, which is smaller than that previously reported.

DOI: 10.1103/PhysRevB.67.193402 PACS number(s): 73.20.At, 68.37.Ef, 72.10.Fk

I. INTRODUCTION

Since the early days of quantum mechanics, the particle-in-a-box problem has always attracted special attention, because it serves to illustrate how the spatial confinement of wave functions leads to quantized electron energy levels. These levels become observable where the dimensions of the quantum box are of the order of the electron wavelength. Examples abound, e.g., in semiconductor quantum wells[1] and in thin metal overlayers.[2,3] A spectacular real-space observation of electron confinement in one and two dimensions has been realized by scanning tunneling microscopy (STM) and scanning tunneling spectroscopy (STS) on the (111) surfaces of noble metals.[4–7] Here, surface-state electrons form a two-dimensional gas scattered by impurities, steps, or islands, and may be confined in artificial structures.

The STM is based on the quantum-mechanical tunneling of electrons, and hence a key issue is to understand what these tunneling measurements represent. Since the seminal theoretical work of Tersoff and Hamann,[8] it has generally been accepted that the tunnel current I at a given tip position (x,y,z) is approximately equal to the integrated local density of states (ILDOS), integrated over the energy range between the sample Fermi level (E_F) and eV, where V is the applied voltage. Accordingly, the differential conductance dI/dV should be approximately proportional to the LDOS at the energy eV, and a constant current topographic image (an STM image) should represent a contour of constant integrated local density of states. For measurements at bias voltages close to E_F, the LDOS and the ILDOS are essentially the same. However, with increasing bias voltage magnitude the STM image should systematically diverge from LDOS (and dI/dV) as states from a range of energies contribute to the integrated state density.

Here, we report on the bias-dependent evolution of the integrated charge density as measured directly in constant current STM images, using an ideal test case of a quantum box consisting of two-dimensional surface states on Ag(111) confined by parallel surface steps. Using dI/dV measurements, Bürgi *et al.*[9] have shown that such a system can be well described as a Fabry-Pérot resonator with partially reflecting walls. However, we find that a simple free-particle model with hard-wall confinement at surface steps[4] is already sufficient to identify all major features in the observed dI/dV maps and, particularly important here, in constant current topographic images, which both result from the superposition of states up to eight allowed subbands. The symmetry of the quantum box allows a direct estimation of the contribution of each state, in contrast to the case of two-dimensional confinement as in corrals, rectangular resonators, or islands.[6,10,11]

The STS measurements performed on large defect-free terraces yield a new value for the surface-state lifetime width $\Gamma = 4.9 \pm 0.2$ meV, which is smaller than that previously measured in STS (Refs. 12 and 13) and in photoemission.[14]

II. EXPERIMENT

The experiments were performed in a home-built STM, operating in ultrahigh vacuum (UHV) at a temperature of 4.8 K.[15] The Ag(111) sample was prepared by repeated cycles of sputtering and annealing. We use electrochemically etched W tips treated in UHV by Ar ion bombardment. Bias voltages are applied to the sample, i.e., positive voltage corresponds to tunneling into unoccupied sample states. Addition of a modulation to the voltage (amplitude $V_{pp} = 1$–10 mV at $\omega = 1.4$ kHz) allows us to record simultaneously constant current images and dI/dV maps and, under open feedback conditions, dI/dV spectra, using a lock-in amplifier.

III. RESULTS AND DISCUSSION

Figures 1(a,b) show atomically resolved STM constant current images, taken at $+21$ and $+6$ mV bias voltages, which on a 18.5-nm-wide terrace simultaneously display a standing wave pattern of the confined surface-state electrons perpendicular to the two parallel step edges. Five maxima

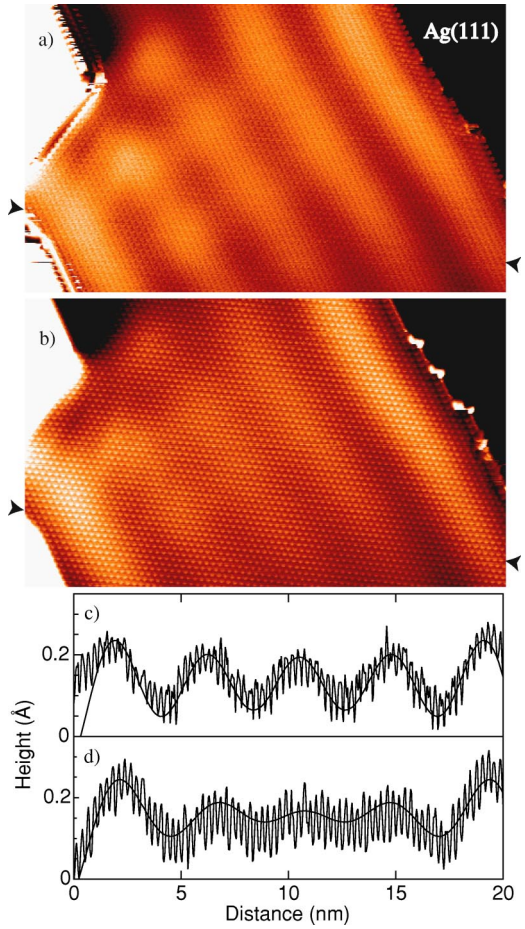

FIG. 1. (Color online) Atomically resolved STM constant current images 20×12 (nm^2), $I=1.8$ nA at (a) $+21$ mV and (b) $+6$ mV showing standing-wave patterns. (c) and (d): cross sections along the black arrows in (a) and (b), respectively, showing the atomic corrugation (small amplitude oscillations) superimposed on the standing waves (large amplitude oscillations). The solid curves following the latter are the calculated ILDOS (see Figs. 3 and 4), taking into account the angle between the normal to the step edge and the direction of the line cut.

are discerned, which are superimposed on the atomic corrugation. The apparent atomic corrugation shown in Figs. 1(c,d), obtained by a cross section along a nearest-neighbor orientation [black arrows in (a) and (b), respectively], is about 0.1 Å, indicating a noise level below 1 pm. This low noise level enables a direct estimation of the perpendicular wave vector of the surface-state electrons.

Figure 2 presents a dI/dV spectrum (dots) measured on a large defect-free terrace [200×200 (nm^2)] showing the characteristic surface-state band onset of width Δ, previously used to estimate the lifetime width $\Gamma=\hbar/\tau$. This geometrical width Δ, which is a combination of intrinsic width Γ, temperature, and modulation broadening, has been related to the self-energy Σ , which in turn corresponds to half the lifetime width: $\Gamma=2\Sigma$ (Ref. 12). Here, the data are of sufficient quality to determine the onset energy and the lifetime width directly from a line-shape analysis (solid curve in Fig. 2). The contribution of the surface-state electrons to the dI/dV signal is described by the steplike density of states,[12,14]

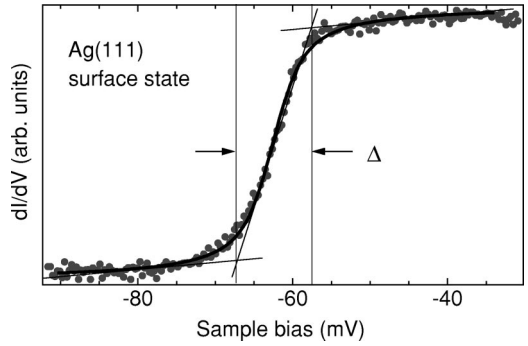

FIG. 2. dI/dV (dots) vs bias voltage V (modulation: $V_{pp}=5$ mV), measured on a large defect-free terrace, showing the steplike onset of the Ag(111) surface state. Solid curve: fit to the data.

$$n(E)=\frac{1}{\Gamma/2}\arctan\left(\frac{E-E_0}{\Gamma/2}\right), \tag{1}$$

where E_0 is the energy position of the surface-state band edge and Γ is the intrinsic width of the surface state. The modulation technique used in STS introduces a broadening of the step which is of the form[16,12]

$$f_{mod}(E)=\frac{\sqrt{(V_{pp}/2)^2-(E-eV)^2}}{(V_{pp}/2)^2}. \tag{2}$$

The thermal broadening, taken into account by the derivative of the Fermi function

$$\frac{df_{Fermi}}{dE}=\frac{1}{2k_BT}\frac{1}{1+\cosh\dfrac{E-E_F}{k_BT}} \tag{3}$$

contributes to the experimentally observed step slope. Since V_{pp} and T are known, the width Γ and the energy position E_0 are obtained by a convolution of the three functions in Eqs. (1)–(3) fitted to the data. Figure 2 shows the fit (full curve) for an average of three measurements, yielding $E_0=-63\pm1$ meV and $\Gamma=4.9\pm0.2$ meV. This new value for Γ is about a factor of 2 smaller than our previous result[12] and about 1 meV smaller than recent results from STS,[13] photoemission,[14] and theoretical predictions.[17] Experimentally, for STS a smaller lifetime width than in photoemission is expected, since the former is measured on locally defect-free surface regions.

Figure 3(a) displays constant current (shaded) and dI/dV (solid curves) cross sections obtained at the indicated bias voltages from a slightly larger quantum box than that in Fig. 1 formed by two parallel steps on Ag(111). Clear oscillations in both, constant current and dI/dV curves are observed,[20] where the number of oscillations increases from bottom to top. The origin of the oscillations is the interference of incident and scattered surface-state electrons at the box boundaries.[4,5,7,18] Due to the boundary conditions given by the confinement in a box of width L, the component of the electron wave vector perpendicular to the step edges $k_\perp$ is

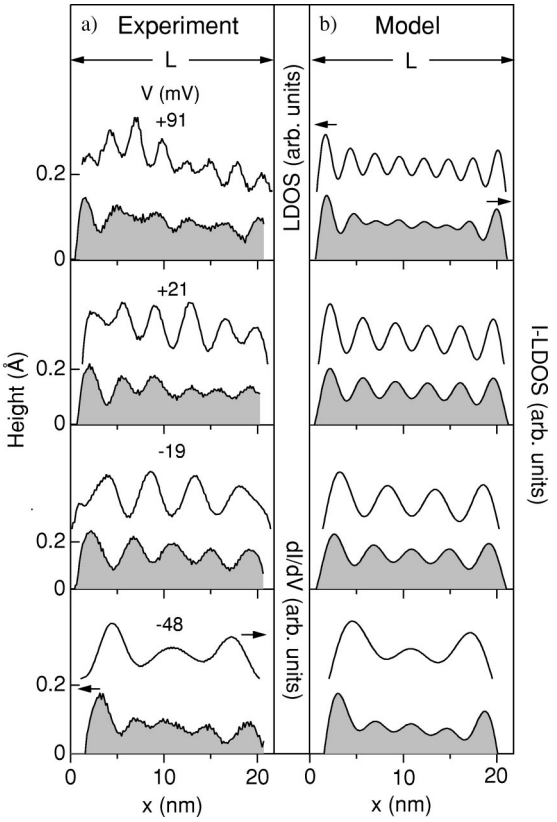

FIG. 3. (a) Simultaneously recorded constant current (shaded) and dI/dV (solid curves) cross sections from a quantum box of width $L=21.8$ nm formed by two parallel steps on Ag(111). Bias voltages are indicated (bias applied to the sample, modulation: $V_{pp}=10$ mV). (b) Calculated electron density [Eq. (6)] and dI/dV.

quantized: $k_{\perp n}=\pi n/L$, with $n>0$. The corresponding wave functions are of the form $\psi_n(x)\propto\sin(k_{\perp n}x)$. The x dependence of $|\psi_n|^2$ is plotted in Fig. 4(a).[21] $E_n(k_{\perp n})$ are the corresponding eigenenergies. Each $E_n(k_{\perp n})$ defines the onset of a one-dimensional subband $E_n(k_\parallel)$, where $E(k)$ is the dispersion relation for the Ag(111) surface-state electrons

$$E(k)=E_0+\frac{\hbar^2k^2}{2m^*}. \tag{4}$$

Figure 4(b) displays $E(k_\perp)$ (solid curve), and the calculated allowed energies $E_n(k_\perp)$ for a quantum box of width $L=21.8$ nm (indicated by open circles). Black dots represent the experimental bias voltages used in the measurements, where the bars denote the modulation ($V_{pp}=10$ mV) added to the bias. As the surface-state electrons are free in the direction parallel to the steps, each one-dimensional subband $E_n(k_\parallel)$ contributes with a DOS of the form $1/\sqrt{E-E_n}$. The total LDOS is then given by

$$D(E,x)\propto\sum_n \frac{|\psi_n(x)|^2}{\sqrt{E-E_n}}, \quad n|\ E_n\leqslant E. \tag{5}$$

In Fig. 4(c), the DOS for the surface-state electrons confined in a box of width $L=21.8$ nm in the x direction and free in the y direction is represented for $n=1$–9. Experimentally,

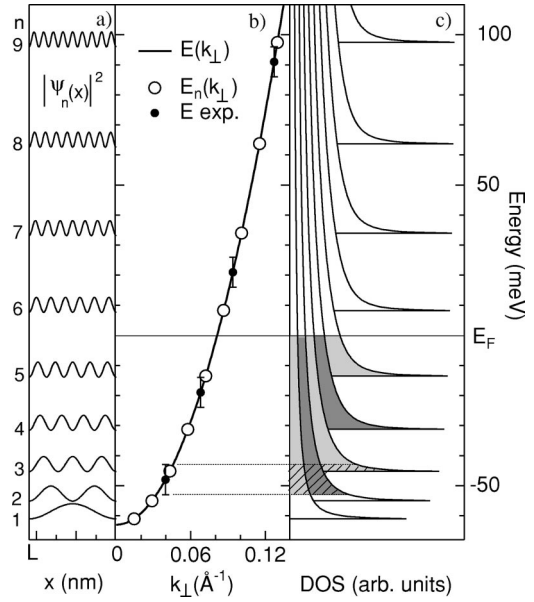

FIG. 4. (a) Calculated $|\psi_n(x)|^2$ for a 1D box of width L. (b) Energy dispersion relation $E(k_\perp)$ for the electrons in the Ag(111) surface state [$E_0=-63$ meV (Fig. 2), $m^*=0.40m_e$ (Ref. 19)]. ○: calculated allowed energies E_n for $L=21.8$ nm, defining the energy onset for the $E_n(k_\parallel)$ subbands; ●: experimental bias voltage (modulation: $V_{pp}=10$ mV, indicated by the error bars). (c) DOS for the surface-state electrons confined in a box of width $L=21.8$ nm: each divergence at $E=E_n$ is followed by a $1/\sqrt{E-E_n}$ decay, corresponding to the $E_n(k_\parallel)$ subband ($n=1$–9) (see text).

the sharp discontinuities in the DOS at each subband onset are broadened by a combination of the applied modulation, partial wall reflectivity,[9] inelastic scattering,[6] and lifetime.

In the simplest approximation of arbitrarily localized tip wave functions,[8] the current I measured by the STM at a tip height z is given by

$$I(V,x)\propto\int_{E_F}^{eV}\sum_n \frac{|\psi_n(x)|^2}{\sqrt{E-E_n}}dE, \quad n|\ E_n\leqslant E, \tag{6}$$

where the integral is taken over the energies between the bias voltage V and E_F. As illustrated in Fig. 4(c), the ILDOS calculated at -48 mV is the superposition of the subbands $E_n(k_\parallel)$ with $n=1$–5. The contribution of each subband $E_n(k_\parallel)$ follows directly from the definition of the current [Eq. (6)]: the weight of each subband $E_n(k_\parallel)$ is given by the integral of the DOS(E_n) from eV to E_F, as indicated by the shaded areas (the modulation is also taken into account). A comparison of the experimental cross section for $V=-48$ mV [Fig. 3(a), bottom] and the model electron density calculated as above [Fig. 3(b), bottom] shows a very good agreement.

The calculation of a model dI/dV also requires an integration of the DOS because of the modulation technique used in the measurements: this is represented in Fig. 4(c), again for the case at -48 mV, as the hatched area around eV. The model shows that the contribution from the subbands with $n=1$, 2, 3 should be found in the experimental dI/dV cross section. A comparison between experiment and

model (Fig. 3) is satisfying. Note the difference between dI/dV (LDOS) (three maxima) and topography (ILDOS) (five maxima) at a tunneling voltage that may be considered to be close to E_F. In both cases, the model calculation takes into account the superposition of the involved states multiplied by an exponential decay function $[\exp(-x/\Lambda)]$ to approximate the effect of asymmetric damping at the quantum box boundaries.[9]

Following the evolution of the standing-wave patterns with increasing bias voltage in Fig. 3, this very good match between measurement and modeling is maintained. The current measurement at -19 mV includes contributions from all five occupied subbands, while the $n=5$ one is excluded from the dI/dV measurement. Note that all subbands with $E_n<eV$ contribute to both LDOS and ILDOS, although the spatial ondulations in the LDOS are dominated by the highest energy included subband. The current and dI/dV measurements performed at $+21$ mV detect the superposition of the same subbands $n=1-6$ with comparable weights in both cases, since the topography and the dI/dV cross sections present similar patterns. Also at $+91$ mV, all subbands with $n=1-8$ participate in both I and dI/dV signals, but for the latter, the $n=8$ one gives the larger contribution.[22] The present data indicate that the difference between dI/dV and topographic measurements can be pronounced already for bias voltages as small as 19 mV. Thus, even close to E_F, the interpretation of constant current images in terms of a simple LDOS may be not fully correct.

The observed standing-wave pattern shown in Fig. 1, obtained from a 18.5-nm-wide quantum box, are analyzed accordingly. At $+6$ and $+21$ mV, the constant current images present five maxima as expected from the model applied to a box of this size [Figs. 1(c,d)]. The different relative contrast between atomic corrugation and standing-wave pattern is due to the changing contribution of the confined wave functions at the two bias voltages.

These comparisons show that we are able to follow in detail the evolution of the confined states over a wide energy range, both in constant current images and in dI/dV maps.

IV. CONCLUSION

To summarize, we measured the lifetime width and the standing-wave patterns of surface-state electrons on Ag(111). The energy dependent standing-wave patterns develop from the superposition of allowed wave functions in the quantum box. A simple free-electron model is already sufficient to identify all major features in differential conductance (dI/dV) maps and constant current images, which both result from the superposition of up to eight allowed states. These results illustrate how the difference between dI/dV and topographic measurements can be pronounced already at very low bias voltages.

ACKNOWLEDGMENTS

This work has been supported by the Swiss National Science Foundation.

[1] L. L. Chang, in *Highlights in Condensed Matter Physics and Future Prospects*, edited by L. Esaki (Plenum, New York, 1991), p. 83.
[2] R.C. Jaklevic and J. Lambe, Phys. Rev. B **12**, 4146 (1975).
[3] J.J. Paggel, T. Miller, and T.-C. Chiang, Science (Washington, DC, U.S.) **283**, 1709 (1999).
[4] M.F. Crommie, C.P. Lutz, and D.M. Eigler, Nature (London) **363**, 524 (1993).
[5] Y. Hasegawa and Ph. Avouris, Phys. Rev. Lett. **71**, 1071 (1993).
[6] M.F. Crommie, C.P. Lutz, and D.M. Eigler, Science (Washington, DC, U.S.) **262**, 218 (1993).
[7] Ph. Avouris and I.-W. Lyo, Science (Washington, DC, U.S.) **264**, 942 (1994).
[8] J. Tersoff and D.R. Hamann, Phys. Rev. B **31**, 805 (1985).
[9] L. Bürgi, O. Jeandupeux, A. Hirstein, H. Brune, and K. Kern, Phys. Rev. Lett. **81**, 5370 (1998).
[10] J. Kliewer, R. Berndt, and S. Crampin, New J. Phys. **3**, 22.1 (2001).
[11] J. Li, W.-D. Schneider, R. Berndt, and S. Crampin, Phys. Rev. Lett. **80**, 3332 (1998).
[12] J. Li, W.-D. Schneider, R. Berndt, O.R. Bryant, and S. Crampin, Phys. Rev. Lett. **81**, 4464 (1998).
[13] J. Kliewer, R. Berndt, E.V. Chulkov, V.M. Silkin, P.M. Echenique, and S. Crampin, Science (Washington, DC, U.S.) **288**, 1399 (2000).
[14] G. Nicolay, F. Reinert, S. Schmidt, D. Ehm, P. Steiner, and S. Hüfner, Phys. Rev. B **62**, 1631 (2000).
[15] R. Gaisch, J.K. Gimzewski, B. Reihl, R.R. Schlittler, M. Tschudy, and W.-D. Schneider, Ultramicroscopy **42-44**, 1621 (1992).
[16] J. Klein, A. Legér, M. Belin, D. Défourneau, and M.J.L. Sangster, Phys. Rev. B **7**, 2336 (1973).
[17] A. Eiguren, B. Hellsing, F. Reinert, G. Nicolay, E.V. Chulkov, V.M. Silkin, S. Hüfner, and P.M. Echenique, Phys. Rev. Lett. **88**, 066805 (2002).
[18] L.C. Davis, M.P. Everson, R.C. Jaklevic, and W. Shen, Phys. Rev. B **43**, 3821 (1991).
[19] J. Li, W.-D. Schneider, and R. Berndt, Phys. Rev. B **56**, 7656 (1997).
[20] Here, tunneling conditions and bias modulation prevent atomic resolution.
[21] As $\lambda=2\pi/k_\perp$, the allowed wavelengths fulfill the condition $\lambda/2=L$. But, as $|\psi_n(x)|^2$ is detected, the observed distance between two consecutive maxima is $\lambda/2$.
[22] The main difference between experimental and model dI/dV arises at the terrace edges, where the measurements are most perturbed by tip-height variations (see Ref. 19).